Studying the metal–support interaction in Pd/γ-Al_2O_3 catalysts by atomic-resolution electron energy-loss spectroscopy

K. Sun[a,*], J. Liu[b], N. Nag[c], and N.D. Browning[a]

[a] *Department of Physics, University of Illinois at Chicago, 845 W. Taylor St., Chicago, Illinois 60607-7059, USA*
[b] *Monsanto Company, 800 N. Lindbergh Blvd., St. Louis, Missouri 63167, USA*
[c] *Process Technology Group, Engelhard Corporation, 23800 Mercantile Road, Beachwood, Ohio 44122, USA*

Received 18 June 2002; accepted 28 August 2002

A 2 wt% Pd/γ-Al_2O_3 catalyst, reduced in hydrogen at different temperatures, has been studied by combined atomic resolution Z-contrast imaging and electron energy loss spectroscopy (EELS) techniques. Z-contrast images have been used primarily to evaluate the particle -size distribution and morphology as a function of the catalyst reduction temperature. Energy-loss spectra obtained from specific locations in and around the metal particles show a shift in the Pd $M_{2,3}$ edge, which is an indication of the Pd nanoparticles getting negatively charged. This acquired charge on the Pd particles is the result of electron transfer from the alumina support and appears to be dependent on the size of the Pd nanoparticles. No aluminum signal is observed on the surface of the metallic nanoparticles, and the observed oxygen signal on the Pd nanoparticles is probably due to oxygen that gets adsorbed on the reduced catalyst.

KEY WORDS: palladium; gamma alumina; supported metal catalysts; reduction process; EELS; Z-contrast imaging; STEM; metal–support interaction (MSI).

1. Introduction

Evidence is emerging to substantiate the idea that a so-called "inert" support, like alumina, upon which metals are often carried to make heterogeneous catalysts, is not really inert, and that the supported catalyst is a system where the support and the active metal could be bound together by well-developed chemical bonds. By carefully preparing alumina- and magnesia-supported Ir clusters, and characterizing them by various spectroscopic tools, including EXAFS, and by model reactions, Gates and coworkers [1,2] have recently demonstrated that there is a distinct chemical bond (0.21 nm) between the Ir atoms of the clusters and the oxygen of the support alumina. Carrier–catalyst interaction has been the subject of investigation for many years, and the "strong metal–support interaction" (SMSI) [3] phenomenon has been studied extensively by various workers over many years. The nature of bonding between active metal and support atoms appears to be the key to the specificity of a supported catalyst in catalyzed reactions.

Supported palladium catalysts are active in the synthesis of methanol [4] and ethanol [5], the removal of NO in environmental catalytic technologies [6], and in methane combustion [7]. It has been found that the activity and selectivity of these Pd catalysts are strongly affected by the support material used [8]. This strongly suggests that an interaction with the support can alter the electronic properties of palladium, and this may happen by some chemical bond formation as mentioned earlier. Although early studies indicated that supported palladium catalysts do not show a strong metal–support interaction [9,10], many experiments have since shown results that can be attributed to the interaction between Pd and alumina. For example, CO can be partially dissociated by Pd clusters supported on both γ-Al_2O_3 [11] and thin aluminium oxide films [12]. Experiments devoted to studying the interaction of a support with supported Pd clusters have suggested various mechanisms. One suggestion is that the "metal–support interaction" (MSI) originates from the formation of Pd–Al alloys at the metal–support interface in Pd/alumina catalysts [13]. However, Baker *et al.* [10] found no sign of an interaction (*i.e.*, the formation of an alloy or the encapsulation of Pd particles by reduced alumina) between Pd and alumina at 1073 K. From the study of model catalysts, *i.e.*, small Pd particles deposited on α-Al_2O_3 and γ-Al_2O_3 substrates, an alternative mechanism has been proposed [10]. From the data obtained by X-ray photoelectron spectroscopy (XPS), Tsud *et al.* [14] attributed the interaction between Pd and γ-Al_2O_3 to electron transfer from the substrate alumina to Pd particles. However, this mechanism has not been tested in practical γ-Al_2O_3-supported Pd catalysts.

In general, the MSI is explained by either a "geometric" (encapsulation or decoration of the metal species by the support oxides, or by sintering of the metal particles on the support) or an "electronic" (a charge transfer between the supported metal and the support)

---

[*] To whom correspondence should be addressed.
E-mail: browning@uic.edu

1011-372X/02/1200-0193/0 © 2002 Plenum Publishing Corporation

phenomenon [15]. Imaging techniques, such as high-resolution electron microscopy (HREM) [16] and scanning tunneling microscopy (STM) [17], have contributed to the studies of the encapsulation or decoration of metal species by supported oxides. Other spectroscopic techniques have also been employed to study the electronic structures of the supported catalysts, including secondary ion mass spectroscopy (SIMS) [18], X-ray photoemission spectroscopy (XPS) [11,14], extended X-ray absorption fine structure (EXAFS), and X-ray absorption near edge spectroscopy (XANES) [19]. While these spectroscopic techniques have provided valuable information on the interactions between the metallic species and the supports, conclusions could not be made directly because these techniques cannot separate the bulk from the interfacial spectra. In addition, it must be expected that electronic and geometric effects frequently overlap.

To fully understand the MSI, it is important to obtain structural and electronic information directly from the interfaces in practical catalysts. Since the metal particles are usually nanometers in size, one needs to combine imaging and spectroscopic techniques to extract both morphological and electronic information. Such a detailed level of analysis is afforded by a combination of atomic resolution electron energy-loss spectroscopy (EELS) [20,21] and Z-contrast imaging [22,23], performed simultaneously in a scanning transmission electron microscope (STEM) [24]. In particular, these techniques can be used to determine particle size, morphology, and changes of the valence and oxidation states of the metal particles, the support, and the metal–support interface at the atomic level.

In the present study, combined EELS and Z-contrast imaging techniques have been used to characterize a Pd/γ-Al_2O_3 catalyst reduced under different conditions. Information on particle size and morphology of palladium species as well as the electronic structure of the catalyst has been evaluated.

2. Experimental procedure

2.1. Catalyst preparation

A gamma alumina (γ-Al_2O_3) powder (BET SA: 160 m^2/g, and Hg pore vol. 2.3 ml/g) was used as the support. Sufficient amount of solution of Na_2PdCl_4 (adjusted to pH = 4) to give a Pd loading of 2 wt% was added dropwise to a 10% aqueous slurry (pH was adjusted to about 11 by sodium carbonate) of the alumina powder. After 30 min of adsorption of the salt the temperature was raised to 338 K and held for 30 min. After complete adsorption of the salt, as indicated by clear filtrate generated from the slurry, the slurry was filtered, washed, and dried overnight at 393 K. Portions of this dry material were reduced at temperatures of 523, 773, and 1073 K. The catalyst was loaded in a tubular furnace and protected by two plugs of quartz wool. A thermocouple was placed in the center of the catalyst bed. The tubular furnace was flushed with nitrogen and then was filled by a flow of 4% H_2 in Ar (40 ml/min). The temperature was slowly raised to the desired final value and held at that temperature for 2 h. The catalyst was then cooled down to room temperature in hydrogen and then discharged into the containers for storage.

2.2. Catalyst characterization

Specimens for electron microscopy analysis were prepared by directly placing the powders on holey-carbon-coated copper grids. Z-contrast imaging and EELS were performed in a JEOL 2010F field emission STEM/TEM operating at 200 kV in STEM mode. The lens conditions of the microscope were defined to form a probe size of 0.2 nm with a convergence angle of 13 mrad and a collection angle of 52 mrad. The energy resolution of the energy-loss spectra is 1.2 eV (defined by the full width at half maximum of zero loss peak) at a dispersion of 0.3 eV/channel. The Gatan PEELS system and EL/P 3.3 software were used for EELS data collection and processing.

Experimentally, the Z-contrast image is formed by collecting the high-angle scattering that is defined by the Rutherford scattering cross-section and is approximately proportional to Z^2 (and hence the name). For the catalyst systems studied here, this means that the image contrast is very sensitive to the presence of Pd (high-Z), and even the smallest clusters, *i.e.*, a single atom [23], can be observed. The incoherent nature of the collected signals means that it can be used to determine the size distribution of the clusters and to determine the position of the interface with the oxide (Note: in conventional TEM this is extremely difficult as the clusters are masked by the substrate and interference effects obscure the image of the interface.) As the image only uses the high-angle scattering, the low-angle scattering can be used simultaneously for EELS [20,21]. Therefore, spectra can be obtained from precise positions in and around the interface between the oxide and the metal cluster (defined by the image). It is these spectra that are used to understand the electronic interactions occurring on a sub-nanometer scale.

3. Results

Figures 1(a–c) show representative Z-contrast images taken from the catalysts reduced at 523, 773, and 1073 K, respectively. These images clearly demonstrate that many small metal clusters (particles) were formed during the reduction of the catalysts. To obtain the particle-size distribution, 200 particles from several images acquired from different areas of several

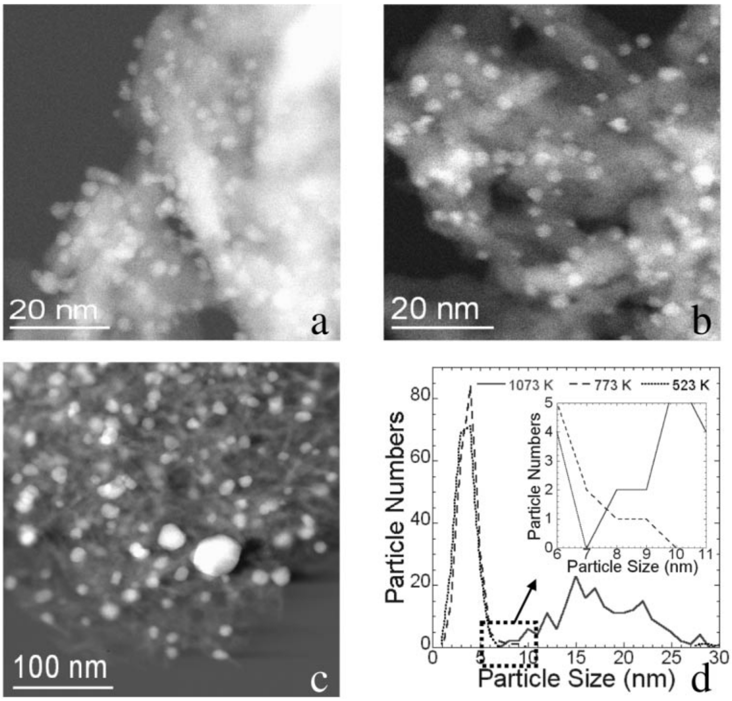

Figure 1. (a), (b) and (c) Z-contrast images of the Pd/γ-Al$_2$O$_3$ catalyst with 2.0 at% Pd loading after reduction at 523, 773 and 1073 K, respectively; (d) the size distribution of Pd crystallites formed at these three different conditions.

specimens of the catalyst reduced at each temperature were examined. The statistical results are shown in figure 1(d), which clearly indicates that most particles have a size less than 7 nm in diameter (in the size range of 2–5 nm) at the reduction temperature of 523 K. Only one particle larger than 7 nm (~28 nm) was observed, which indicates that it is the particles that are smaller than 7 nm that are overwhelmingly responsible for the properties of the catalyst at this reducing temperature. The overall size distribution of the catalyst reduced at 773 K is different from that of the catalyst reduced at 523 K; the average particle size is increased slightly in the former. One particle in the range of 7–9 nm and one very large particle (~70 nm) were observed in this representative distribution (as opposed to just one single particle when the sample was reduced at 523 K).

At the reduction temperature of 1073 K, the particle-size distribution is dramatically altered. Probably because of sintering at these high temperatures, most of the particles have grown into the size range of 7–30 nm with several very large particles (>30 nm) also being observed. Unlike the samples reduced at lower temperatures, the particle-size distribution in the sample reduced at 1073 K is very wide. Furthermore, many particles are faceted with flat surfaces, which is significantly different from those samples reduced at lower temperatures.

Figure 2(a) shows a higher magnification Z-contrast image of the catalyst reduced at 523 K, in which a

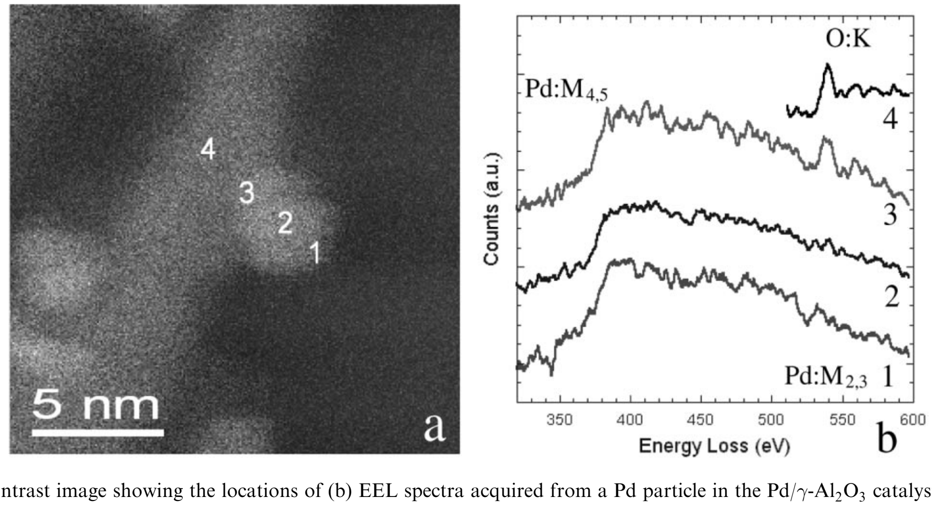

Figure 2. (a) Z-contrast image showing the locations of (b) EEL spectra acquired from a Pd particle in the Pd/γ-Al$_2$O$_3$ catalyst reduced at 523 K.

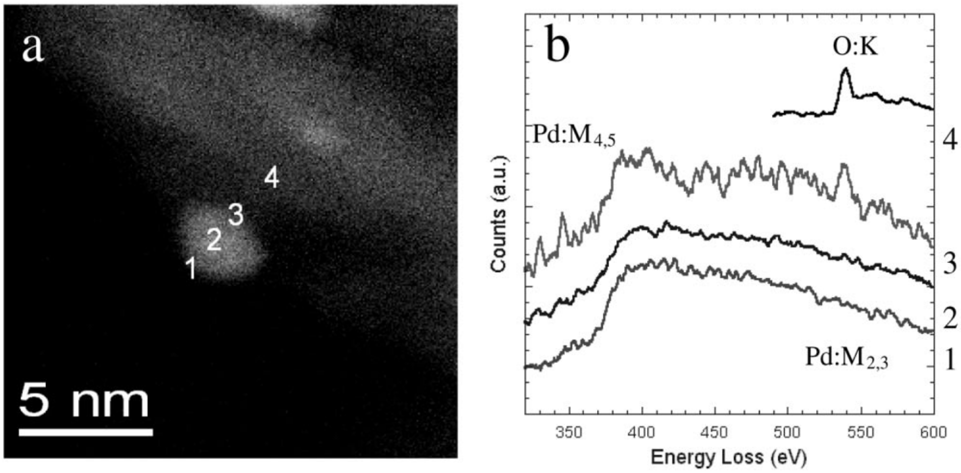

Figure 3. (a) Z-contrast image showing the locations of (b) EEL spectra acquired from a Pd particle in the Pd/γ-Al_2O_3 catalyst reduced at 773 K.

small particle coexisting with an alumina crystal is clearly observed. Energy-loss spectra acquired from the positions marked in figure 2(a) are shown in figure 2(b). The background in these displayed spectra was subtracted using standard methods [25], and was smoothed and normalized to the continuum interval between 570 and 600 eV. The spectra were also shifted vertically for clearly displaying the spectra. Spectra 1 and 2 were acquired from the surface and center of a particle. Within this energy-loss range, the spectra consist of delayed Pd $M_{4,5}$ (for metallic Pd with onset at 335 eV) and the $M_{2,3}$ (at 532.3 eV for metallic Pd) edges, or the oxygen K-edge (onset at around 532 eV). It is obvious that the Pd $M_{2,3}$ edges overlap with the oxygen K-edge, which makes the identification of the oxidation state of the Pd particles difficult. Nevertheless, no obvious peaks showing up at around 532 eV in the two spectra suggests that this particle is primarily composed of metallic Pd (similar spectra are obtained from all the particles studied in this sample). Comparing spectrum 3, which was acquired from the interface between the particle and the support, with spectrum 4, which is acquired from the support, we can see that there is no obvious chemical shift of the oxygen K-edge or Pd $M_{2,3}$ edges in the interface spectrum. This is the case for all interfaces studied, except for the large particle mentioned earlier, where a 4.8 eV negative chemical shift was observed in the $M_{2,3}$ interface spectrum. (This will be discussed in more detail later.)

Figure 3(a) shows a high magnification Z-contrast image of the catalyst reduced at 773 K in which a Pd particle attached to the alumina support is again clearly shown. Energy-loss spectra acquired from the positions marked in figure 3(a) are shown in figure 3(b). These spectra are processed in the same manner as described above. Spectra 1 and 2, which are acquired from the surface and the center of the particle, respectively, show features representing metallic Pd. This again suggests that the small clusters formed at this temperature can be metallic Pd. As with the analysis of the sample reduced at 523 K, there is no observable shift of the oxygen K edge (or Pd $M_{2,3}$ edges) for the interfacial spectrum 3 relative to the spectrum 4 of the support. However, similar to the sample reduced at 523 K, chemical shifts larger than 2.4 eV were observed in the spectra that were acquired at the interfaces between large particles and the alumina support.

Figure 4(a) shows a high-magnification Z-contrast image of the catalyst reduced at 1073 K. Here the particle sizes are much larger than those in the previous two specimens. Figure 4(b) shows EELS spectra acquired from the corresponding positions marked in figure 4(a). The spectra (1 to 3) acquired from the large particle indicate that it is metallic Pd. However, spectrum 4 is noticeably different from the first three spectra. The onset of oxygen K-edge (or Pd $M_{2,3}$ edges) exhibits a shift from 532 eV (or 532.3 eV) in the support spectrum (spectrum 5) (or in the metallic Pd spectrum) to 528.4 eV in the interface spectrum (spectrum 4). These large chemical shifts (*i.e.*, larger than 2.4 eV) are the same as have been observed in the interfacial spectra acquired from the interfaces involving larger particles in the previous specimens. Figure 4(c) shows only the oxygen K-edges (Pd $M_{2,3}$ edges) of the interface spectrum along with reference spectra from PdO, together with γ-Al_2O_3 (spectrum 5) and a spectrum that is a combination of the PdO and γ-Al_2O_3. It is observed that the full-width at half-maximum (FWHM) of the main peak in spectrum 4 is larger than those of the reference spectra and it has a 3.6 eV negative shift in the edge onset. The fact that the fine-structure of the interface spectrum is similar to the addition of the PdO and γ-Al_2O_3 spectra suggests that this shift is due to a downward shift of the Pd $M_{2,3}$ edge (which overlaps with the oxygen edge).

Figure 5 shows the sum of the spectra obtained from the surfaces of several different positions of a large particle, together with the PdO reference spectrum and the sum of spectra from several positions at the center

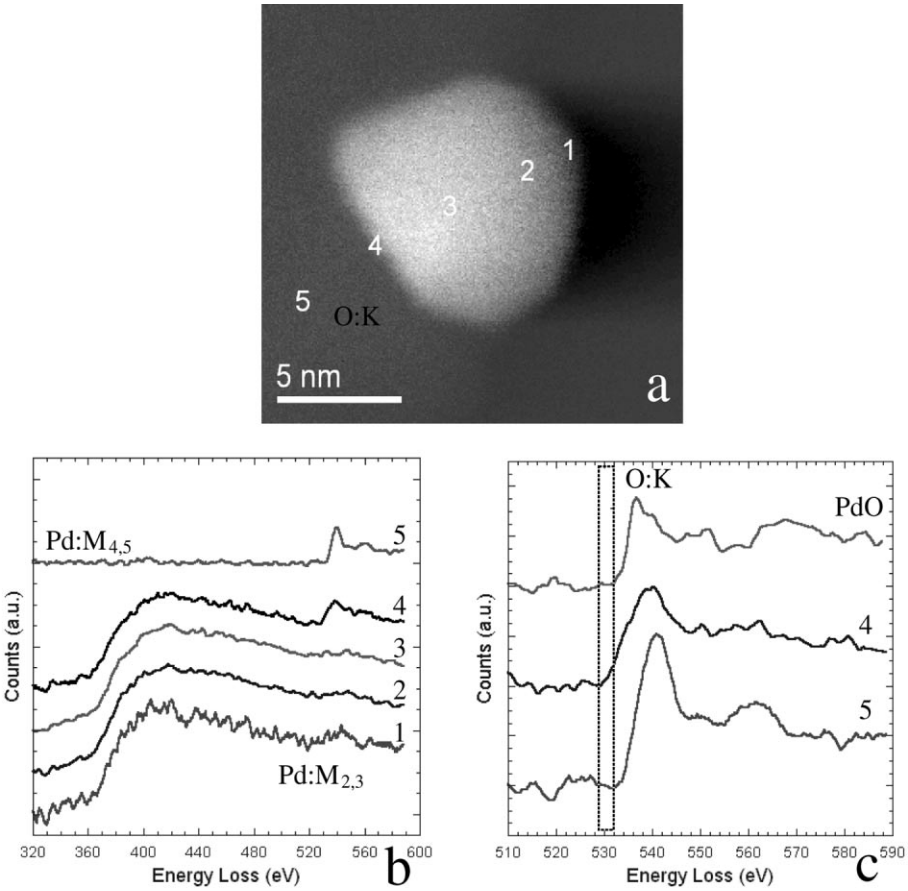

Figure 4. (a) Z-contrast image showing the locations of (b) EEL spectra acquired from a Pd particle in the Pd/γ-Al_2O_3 catalyst reduced at 1073 K; (c) oxygen K-edges of the interface spectrum 4, the support spectrum 5 and a spectrum acquired from PdO.

of the particle. It should be noted that no Al L-edge (at ~70 eV) was observed on the surface of the clusters, indicating that there is no γ-Al_2O_3 decorating the particles. Also, the absence of the first main peak in the spectrum is consistent with the lack of γ-Al_2O_3. Here we can clearly see that the spectrum shows a negative shift (about 4.2 eV or so) from that of PdO. From both the imaging and EELS analysis, we did not find the surface encapsulation of this Pd particle by the support material, which indicates that the observed change is again due to a shift in the onset of the Pd $M_{2,3}$ edge.

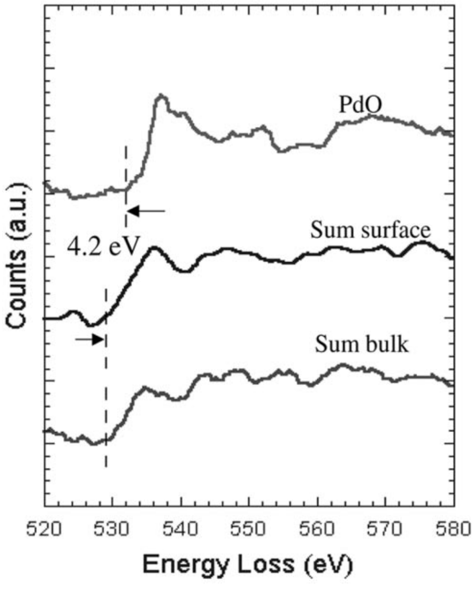

Figure 5. The summed surface and bulk EEL spectra acquired from several different sites of a large particle formed at the reduction temperature of 1073 K together with the PdO reference spectrum.

4. Discussion

The above results show that there exist chemical shifts in the spectra acquired from the interfaces between larger (>10 nm) Pd particles and the support. Since these chemical shifts to lower band-energy (BE) are much larger than the resolution of the spectrometer (±1.2 eV), they cannot be due to experimental uncertainties (and no obvious shifts are observed for the smaller particles). The large chemical shift may be due to a strong interaction between the support and the metal nanoparticle, the occurrence of which is also size-dependent. The amount of the edge shifts is much larger than those found in Al–Pd alloys, namely, 1.73–1.9 eV for AlPd and 2.5 eV for Al_3Pd [26], indicating that the observed shifts are not due to the formation of Al–Pd alloys. Furthermore, the shifts appear not to be due to the oxidation of Pd, as the Pd $3d_{5/2}$ binding energy for metallic Pd is smaller than that for PdO [27,28]. This indicates that if Pd was oxidized, the Pd $3d_{5/2}$ binding energy would shift to a higher energy, but the reverse was observed experimentally. Moreover, calculations of the electronic structure of Pd–alumina interfaces also showed that the Pd–O interaction is relatively weak, while the Pd–Al interaction plays a more important role in metal–alumina bonding [29].

The negative shift of palladium binding energy therefore suggests that the Pd particles are negatively charged. This may be due to the charge transfer from the support to the Pd particles during the reduction process, a mechanism that is consistent with general chemistry principles [30]. When an oxide, denoted by M–O (M is cation in the oxide), is oxygen-deficient, it acts as electron donor and induces the strong bonding with metals deposited on its surface if the deposited metal has a higher electronegativity than M. This is precisely the case in the alumina supported Pd system where Pd has a higher electronegativity (2.2) than Al (1.5) [30] and the surface of γ-Al_2O_3 is generally accepted to contain oxygen vacancies [31]. This means that the support can act as an electron donor to the Pd particles resulting in negatively charged Pd clusters. This is consistent with the model study that describes the MSI resulting from a partial electron transfer from the substrate to Pd [14]. The formation of negatively charged Pd particles induced by the MSI has also been reported in Pd/α-Al_2O_3 (with the addition of ZrO_2) [32] and Pd/La_2O_3 catalysts [8].

The size dependence of the chemical shifts is consistent with the study of the Pd/La_2O_3 [8] catalysts. However, in our study it can also be possible that the size dependence is simply due to the significantly decreased signal-to-noise ratio in the spectra acquired from the very small Pd nanoparticles. An alternative explanation could be that the particles must reach a certain size for particular crystallographic planes to develop at the interface. This is clearly an interesting observation that warrants further detailed experiments. Further experiments are also required to investigate the general applicability of these results to samples with different Pd loadings and to transition metal catalysts.

It should be noted that the STEM analysis performed here typically involves much lower electron doses than those used in conventional TEM techniques. Furthermore, to avoid the occurrence of beam-induced artifacts, all the spectra reported here were acquired from Pd particles viewed at relatively lower magnifications and very short spectrum acquisition times were used. Thus, to our knowledge, electron beam damage, which could be an issue [33], was not responsible for the results discussed here. Furthermore, sequential spectra recorded from the same particle showed identical results. When the catalyst sample was intensively irradiated under an electron beam for a prolonged time, however, the catalyst structure can be significantly modified. The low dose in the STEM probe also avoids the possibility of charging effects in the alumina giving rise to the experimentally observed shifts in the core-edges.

5. Conclusions

In summary, we have studied a Pd/γ-Al_2O_3 catalyst reduced at three different temperatures by atomic resolution *Z*-contrast imaging and electron spectroscopy techniques. The results reported here show that small metallic Pd particles are formed when the catalyst is reduced at lower temperatures. With increasing reduction temperature, the Pd particles grow in size and some large particles may become negatively charged; the charge transfer is proposed to be induced by a strong MSI that occurs between the larger metallic Pd clusters and the oxygen-deficient alumina support. The observed experimental result of a large chemical shift is interpreted as a result of electron transfer from the alumina support to large Pd particles. Thus the results reported in this work are in accord with those of Gates and coworkers [1], that bond formation is possible between the supported metal and the support in a supported catalyst. The size dependence of the chemical shift is certainly interesting and may have a profound effect on the understanding of the performance of supported metal catalysts. We will perform a more detailed study on different systems to understand the nature of this phenomenon.

Acknowledgments

This research was supported by the Monsanto Company and the Petroleum Research Fund under grant number 37552-AC5. The JEOL 2010F STEM/TEM used in this research was partially funded by NSF through Grant DMR-9601792 and is operated by the research resources center (RRC) at UIC.

References

[1] A.M. Argo, J.F. Coellner, B.L. Phillips, G.A. Panjabi and B.C. Gates, J. Amer. Chem. Soc. 123 (2001) 2275.
[2] O. Alexeev, G. Panjabi and B.C. Gates, J. Catal. 173 (1998) 196.
[3] S.J. Tauster, S.C. Fung and R.L. Garten, J. Amer. Chem. Soc. 100 (1978) 170.
[4] M.L. Poutsma, L.F. Elek, P.A. Ibarbia, A.P. Risch and J.A. Rabo, J. Catal. 52 (1978) 157.
[5] P. Forzatti, E. Tronconi and I. Pasquon, Catal. Rev. Sci. Eng. 33 (1991) 109.
[6] G. Centi, J. Mol. Catal. A 173 (2001) 287.
[7] K. Almusaiteer and S.S.C. Chuang, J. Catal. 184 (1999) 189.
[8] T.H. Fleisch, R.F. Hicks and A.T. Bell, J. Catal. 87 (1984) 398.
[9] G.L. Haller and D.E. Resasco, Adv. Catal. 35 (1989) 173.
[10] R.T.K. Baker, E.B. Prestridge and G.B. McVicker, J. Catal. 89 (1984) 422.

[11] I. Stará and V. Matolín, Surf. Sci. 313 (1994) 99.

[12] D.R. Rainer, M.C. Wu, D.I. Mahon and D.W. Goodman, J. Vac. Sci. Technol. A 4 (1996) 1184.

[13] D. Łomot and Z. Karpiński, Catal. Lett. 69 (2000) 133.

[14] N. Tsud, V. Johánek, I. Stará, K. Veltruská and V. Matolín, Surf. Sci. 467 (2000) 169.

[15] K. Hayek, M. Fuchs, B. Klötzer, W. Reichl and G. Rupprechter, Top. Catal. 13 (2000) 55.

[16] S. Bernal, R.T. Baker, A. Burrows, J.J. Calvino, C.J. Kiely, C. López-Cartes, J. A. Pérez-Omil and J.M. Rodriguez-Izquierdo, Surf. Interface Anal. 29 (2000) 411.

[17] O. Dulub, W. Hebenstreit and U. Diebold, Phys. Rev. Lett. 84 (2000) 3646.

[18] E. Gillet, M.H. El Yakhloufi, J.-P. Disalvo and F. Ben Abdelouahab, Surf. Sci. 419 (1999) 216.

[19] J.T. Miller, B.L. Mojet, D.E. Ramaker and D.C. Koningsberger, Catal. Today 62 (2000) 101.

[20] N.D. Browning, M.F. Chisholm and S.J. Pennycook, Nature 366 (1993) 143.

[21] P.E. Batson, Nature 366 (1993) 727.

[22] M.M.J. Treacy, A. Howie and C.J. Wilson, Phil. Mag. A 38 (1978) 569.

[23] P.D. Nellist and S.J. Pennycook, Science 274 (1996) 413.

[24] E. Jimes and N.D. Browning, Ultramicroscopy 78 (1999) 125.

[25] R.F. Egerton, *Electron Energy Loss Spectroscopy in the Electron Microscope*, 2nd edition (Plenum, New York, 1996).

[26] F.U. Hillerbrecht, J.C. Fuggle, P.A. Bennett, Z. Zolnirek and Ch. Freiburg, Phys. Rev. B 27 (1983) 2179.

[27] M. Brun, A. Berthet and J.C. Bertolini, J. Electron Spectrosc. Relat. Phenom. 104 (1999) 55.

[28] E.H. Voogt, A.J.M. Mens, O.L.J. Gijzeman and J.W. Geus, Surf. Sci. 350 (1996) 21.

[29] M. Kohyama, S. Kose, M. Kinoshita and R.R. Yamamoto, J. Phys. Chem. Solids 53 (1992) 345.

[30] B. Ealet and E. Gillet, Surf. Sci. 367 (1996) 221.

[31] S. Soled, J. Catal. 81 (1983) 252.

[32] Y. Lee, Y. Inoue and I. Yasumori, Bull. Chem. Soc. Jpn. 54 (1981) 3711.

[33] K. Heinemann and H. Poppa, Ultramicroscopy 17 (1985) 213.